Journal of Colloid and Interface Science 660 (2024) 1030–1038

Contents lists available at ScienceDirect

Journal of Colloid And Interface Science

journal homepage: www.elsevier.com/locate/jcis

Regular Article

Celecoxib-hydroxypropyl-β-cyclodextrin inclusion complex in a chitosan/PEO-PPO-PEO block copolymer matrix: Structural effect and drug release

Valentino Laquintana [a], Angela A. Lopedota [a], Marianna Ivone [a], Nunzio Denora [a], Massimo Franco [a], Gerardo Palazzo [b,c], Luigi Gentile [b,c,*]

[a] Department of Pharmacy, Pharmaceutical Sciences, University of Bari Aldo Moro, Orabona 4, 70126 Bari, Italy
[b] Department of Chemistry, University of Bari Aldo Moro, Orabona 4, Bari 70126, Italy
[c] Center of Colloid and Surface Science (CSGI) Bari Unit, via della Lastruccia 3, Sesto Fiorentino 50019, Italy

GRAPHICAL ABSTRACT

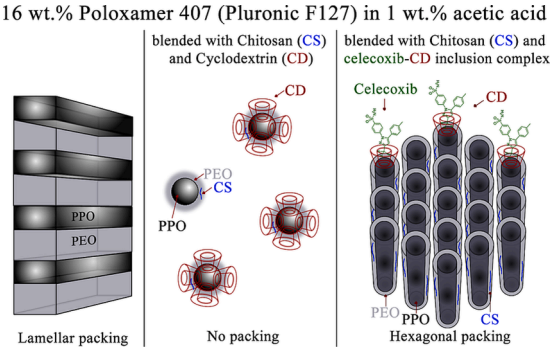

ARTICLE INFO

Keywords:
Block copolymer
Rheology
SAXS
Thermogelation
Inclusion complex
Anti-inflammatory

ABSTRACT

Hypothesis: Triblock copolymers of poly(ethylene oxide) and poly(propylene oxide)-based matrices, such as Poloxamer 407 (P407) or Pluronic® F127, are extensively utilized in drug delivery and permeation systems due to their FDA approval and listing in the US and European Pharmacopoeias. The study hypothesizes that incorporating 2-hydroxypropyl-β-cyclodextrin (HP-β-CD) and the celecoxib-HP-β-CD inclusion complex into a 16 wt% P407 and chitosan blend in an aqueous acetic acid solution will affect the system's rheological and structural properties.

Experiments: Rheological, small-angle X-ray scattering (SAXS), and dynamic light scattering (DLS) experiments were conducted to assess the impact of acetic acid and chitosan on the 16 wt% P407 and chitosan blend. Additionally, *in vitro* drug release studies were performed to monitor the drug release profile over time.

Findings: The addition of HP-β-CD was found to inhibit gel formation in the 16 wt% P407 and chitosan blend. However, the presence of the celecoxib-HP-β-CD inclusion complex showed no significant structural effects compared to P407 blended with chitosan alone. Rheological and SAXS analyses demonstrated that acetic acid led to the formation of a lamellar phase due to the lower pH, facilitating injectability. The presence of chitosan in acetic acid resulted in the detection of a hexagonal phase, affecting the release of celecoxib.

* Corresponding author at: Department of Chemistry, University of Bari Aldo Moro, Orabona 4, Bari 70126, Italy.
E-mail address: luigi.gentile@uniba.it (L. Gentile).

https://doi.org/10.1016/j.jcis.2024.01.019
Received 28 October 2023; Received in revised form 28 December 2023; Accepted 3 January 2024
Available online 11 January 2024

Table 1
All the samples under investigation are listed and the chemical composition is indicated.

Label	P407 (wt.%)	Chitosan (CS) in acetic acid (wt.%)	HP-β-CD (CD) (wt.%)	Celecoxib-CD complex (wt.%)	Description	pH
P407	16	0	0	0	16 wt% of P407 in water	7.1 ± 0.2
P407Ac	16	0	0	0	16 wt% of P407 in an aqueous solution of 1 wt% acetic acid	3.1 ± 0.5
P407CS	16	0.5	0	0	16 wt% of P407 blended with 0.5 wt% of CS in an aqueous solution of 1 wt% acetic acid	3.9 ± 0.2
P407CS-CD	16	0.5	1.68	0	16 wt% of P407 blended with 0.5 wt% of CS and 1.68 wt% of CD in an aqueous solution of 1 wt% acetic acid	3.9 ± 0.2
P407CS-CEX	16	0.5	0	0	16 wt% of P407 blended with 0.5 wt% of CS and added of CEX (1.27 mg/mL).	3.9 ± 0.2
P407CS-CiCD	16	0.5	0	1.68	16 wt% of P407 blended with 0.5 wt% of CS and 1.68 wt% of CiCD in an aqueous solution of 1 wt% acetic acid	3.9 ± 0.2

1. Introduction

The block copolymers have been extensively researched as reliable agents for targeted drug delivery and gene therapy [1–4]. Pluronic block copolymers with a triblock poly(ethylene oxide)$_x$-poly(propylene oxide)$_y$-poly(ethylene oxide)$_x$ structure abbreviated as PEO-PPO-PEO, particularly Poloxamer 407 (P407), known as Pluronic® F127 (x = 97, y = 69), have gained attention for controlled drug delivery due to their ability to undergo a tunable and thermo-reversible sol–gel transition. This transition occurs from a micellar solution L1 (sol) to a cubic phase (gel), establishing a stable gel phase at body temperature [3,5–13]. The Poloxamer sol-to-gel transition is due to a disorder-to-order transition occurring at concentrations equal to or higher than 15 wt% as a function of temperature [10,11,14,15]. The micellization process and phase diagram of pure Poloxamer 407 (P407) in water depend on copolymer concentration, temperature, and additives [10,11,14,16,17]. Several experimental techniques have been adopted to characterize Poloxamer 407 phase behavior in water, including differential scanning calorimetry (DSC), static and dynamic light scattering (SLS and DLS), small-angle neutron scattering (SANS), small-angle X-ray scattering (SAXS), rheology, and surface tension measurements [10,11,14,16–22]. Specifically, as the temperature increases, an isotropic micellar phase transforms into a face-centered cubic (FCC) packing of the spherical micelles (up to 25 wt%) [19–21]. With further concentration increase, a transition from FCC-to-body-centered cubic (BCC) occurs, passing through a coexistence regime [19,20]. At a concentration higher than 60 wt% in water, a hexagonal phase coexists with a lamellar phase at concentrations above 80 wt%, while values higher than 90 wt% show a lamellar phase [19].

The size of the P407 micelles and their phase behavior in water undergo dramatic changes in the presence of certain additives. Loose large aggregates or clusters are usually observed in these block copolymer systems below their corresponding CMC/CMT due to the presence of more hydrophobic triblock/diblock copolymer chains (sometimes denoted “impurities”) [23]. When the anionic surfactant sodium dodecyl sulfate (SDS) is present with P407, it leads to the formation of mixed micelles [16,17,24–27]. Another type of additive, such as single-walled carbon nanotubes, causes variations in the phase diagram. In the case of nanotubes, a hexagonal phase can be observed between 20 and 25 wt% of P407 [19]. Hydrophobic drug molecules can interact with the core, made of PPO, of the Poloxamer micelles, forming micellar block copolymer-drug complexes. The hydrated coronas of the Poloxamer micelles, composed of PEO, are nontoxic and prevent the drug molecules from being removed from the core, thus increasing the solubility of hydrophobic drugs and enhancing their bioavailability [28].

Chitosan (CS) can be used to enhance the bioadhesive properties of P407 [29]. The cationic polysaccharide CS is obtained from chitin, a natural polymer, with positive charges in its structure, providing excellent bioadhesive characteristics. Furthermore, CS exhibits excellent biocompatibility, biodegradability, and non-toxic properties [30,31]. The impact of chitosan on the critical micellization temperature (CMT), critical gelation temperature (CGT), and dissolution behavior of P407 aqueous solutions has been investigated [32,33]. Acetic acid (Ac) is required to dissolve chitosan, and consequently, a solution of CS/Ac is introduced into the P407/water system. In the case of 20 wt% P407, the CGTs of mixtures containing 0 %, 0.2 %, and 0.5 % CS/Ac are slightly increased compared to P407 alone in water [32,33]. Generally, the literature reports that CS/Ac causes only minor changes in the gelation temperature of the 20 wt% aqueous P407 system. However, the addition of CS/Ac to 18 wt% and 17 wt% P407 leads to a more significant increase in the CGT (3–4 °C). Nevertheless, there has been no in-depth investigation into the effect of Ac on the thermogelation of P407. Therefore, this study will also explore the impact of Ac on the P407/water system.

Cyclodextrins (CD), such as 2-hydroxypropyl-β-cyclodextrin (HP-β-CD), have been utilized as excipient in pharmaceutical formulations due to their ability to form inclusion complexes with poorly soluble drugs [34,35]. Some studies have investigated the interaction between CD and Poloxamers [36–42]. However, only a few studies have considered the potential interactions between CD inclusion complexes and Poloxamer-based binary systems with different hydrophilic-lipophilic balances [43–46]. Valero et al. investigated the impact of CD as a micellization-modulator for P407 micelles loaded with salicylic acid at pH = 1 across various temperatures [47].

Using SAXS, it has been observed that the cluster dimension of 18 wt % P407 decreases in the presence of HP-β-CD, while an increase in the cluster dimension has been reported in the presence of the HP-β-CD inclusion complex, where the hydrophobic cavity is occupied by budesonide [43]. Similar behavior was also observed for 20 wt% P407, with a decrease in cluster size in the presence of HP-β-CD, remaining similar after inclusion complex incorporation (31). The reduction of cluster size when HP-β-CD is present suggests an interaction between the hydrophobic cavity of HP-β-CD and the PPO. Conversely, when the HP-β-CD hydrophobic cavity is already loaded with budesonide, it affects the interactions between the Poloxamer micelles [43].

The interaction between HP-β-CD and the celecoxib-HP-β-CD inclusion complex on a Poloxamer matrix is intrinsically related to drug release, but it becomes more complex when chitosan (CS) in acetic acid (Ac) is added to enhance the bioadhesive properties of the gels. This study elucidates the effect of acetic acid on the order–disorder transition of 16 wt% P407 in water, as well as the impact of CS on the packing process that leads to gel formation at 37 °C, using rheology and SAXS. Furthermore, the effect of HP-β-CD and the celecoxib-HP-β-CD inclusion complex on the P407CS blend and the relative celecoxib release were investigated. The size distribution of the HP-β-CD and celecoxib-HP-β-CD inclusion complex in an aqueous solution of 1 wt% acetic acid was investigated using DLS.

2. Materials and methods

2.1. Materials

The Poloxamer 407, known as Pluronic® F127, a triblock copolymer made of poly(ethylene oxide)$_{97}$-poly(propylene oxide)$_{69}$-poly(ethylene oxide)$_{97}$, was obtained from BASF (Ludwigshafen, Germany) and used without further purification. Hydroxypropyl-β-Cyclodextrin (HP-β-CD) (degree of substitution 7.5) was generously provided by Farmalabor (Canosa, Italia). Reagent grade chemicals, including low-viscosity chitosan (CS) (50 kDa MW), Celecoxib (CEX), and acetic acid solution (96 %), were purchased from Sigma-Aldrich.

2.2. Preparation of HP-β-CD and the celecoxib inclusion complex

The CEX-HP-β-CD (CiCD) inclusion complex was made starting from a 1 % v/v aqueous solution of acetic acid containing 1.68 % by weight of HP-β-CD. Then an excess of CEX was added and the suspension was allowed to equilibrate at room temperature for 48 h under constant magnetic stirring to allow for the interaction between CEX and HP-β-CD. After this time, the mixture was filtered through a 0.45 μm CA filter and the CEX loaded into the inclusion complex was determined by HPLC, following the procedure described below.

2.3. Formulations

The Poloxamer 407, referred to as P407, was prepared at a concentration of 16 wt% in distilled water or in an aqueous solution of 1 wt% acetic acid (P407Ac). The samples were prepared using the cold procedure: the desired polymer and aqueous solutions were weighed and placed in vials with a small magnetic stirrer, then stored at 4 °C.

The P407 systems were blended with chitosan (CS) and subsequently with 2-hydroxypropyl-β-cyclodextrin (HP-β-CD) and the celecoxib-HP-β-CD inclusion complex (CiCD). In the P407CS formulation, 0.5 wt% of chitosan was first dissolved in an aqueous solution of 1 % v/v acetic acid at room temperature. Then, the temperature was lowered to 4 °C, and an exactly weighed quantity of P407 was added to reach a content of 16 wt %. The P407CS-CD and P407CS-CEX formulations were prepared following the above P407CS formulation, with the addition of HP-β-CD at 1.68 wt% for P407CS-CD or the addition of CEX (1.27 mg/mL) for P407CS-CiCD. For both formulations, the addition of HP-β-CD or CEX occurred after complete dissolution of chitosan at r.t., before dissolving P407 at 4 °C.

Lastly, for the P407CS-CiCD formulation, in the solution of inclusion complex (CiCD) 0.5 wt% of chitosan was added, and the temperature was lowered to 4 °C before adding 16 wt% of P407.

All the prepared samples are listed in Table 1.

2.4. Rheology

Rheological measurements were conducted using the MCR302e stress-controlled rheometer (Anton Paar Gmbh, Graz, Austria) equipped with a Taylor-Couette geometry, specifically, concentric cylinder geometry with an inner diameter of 16.662 mm and a gap of 0.704 mm. The temperature was controlled using a Peltier system, and a water circulator apparatus (±0.2 °C) controlled the reference temperature. Two types of dynamic shear experiments were performed: frequency sweep and dynamic temperature sweep tests. All experiments were performed in the linear viscoelastic regime, previously tested by an amplitude sweep test [48].

The storage modulus, G′, and the loss modulus, G″, were collected as a function of the angular frequency from 0.1 to 100 rad/s in the

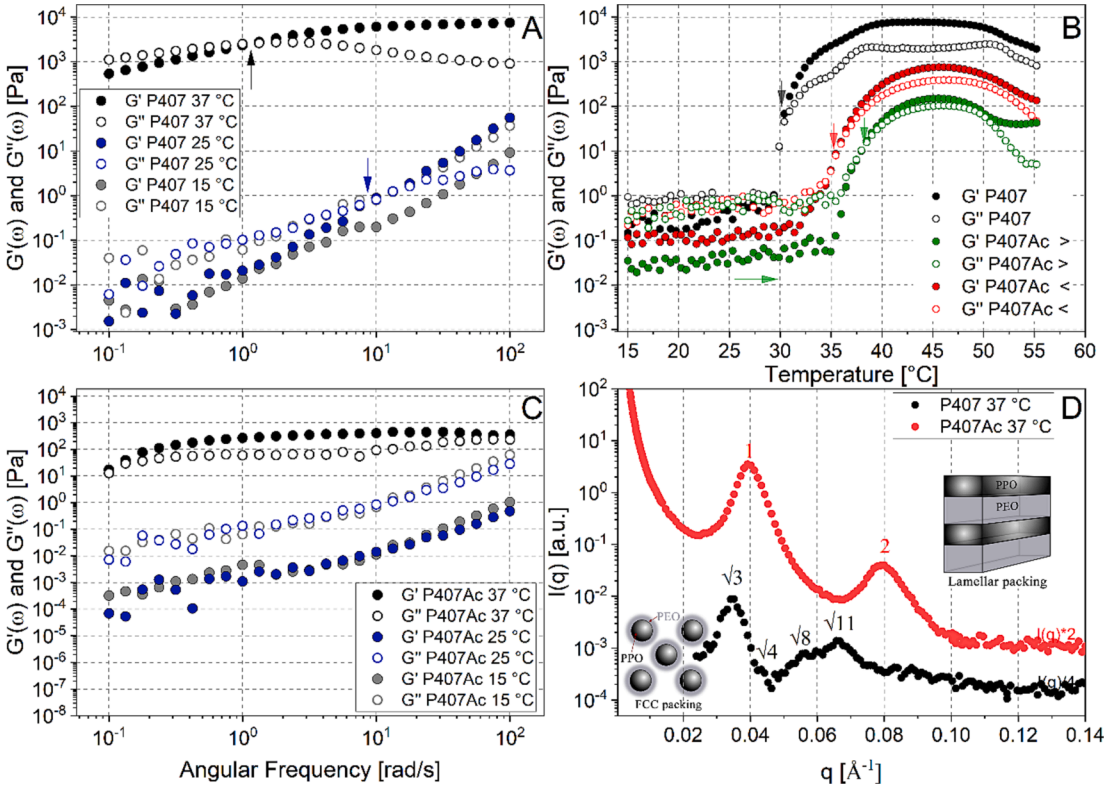

Fig. 1. Frequency sweep tests were performed to measure the storage modulus, G′, and loss modulus, G″, of Poloxamer 407 at 16 wt% in water (P407) at 15, 25, and 37 °C (A). Dynamic temperature sweep tests were conducted from 15 to 55 °C for P407 and the corresponding temperature test for P407 at 16 wt% in a 1 wt% aqueous solution of acetic acid (P407Ac) is shown in green color, followed by cooling down and ramping up again, shown in red color (B). Frequency sweep tests of P407Ac at 15, 25, and 37 °C were performed after the ramp tests (C). The small-angle X-ray scattering intensity, *I(q)*, as a function of the scattering wave vector, *q*, for P407 and P407Ac was collected at 37 °C after dynamic temperature sweep tests (D).

frequency sweep experiments. The Maxwell model can be adopted to provide a correlation between G′ and G″ and the angular frequency [49,50]

$$G^{'}(\omega) = G_0 \frac{\omega^2\tau^2}{1+\omega^2\tau^2} \quad (1)$$

$$G^{''}(\omega) = G_0 \frac{\omega\tau}{1+\omega^2\tau^2} \quad (2)$$

where G_0 represents the storage modulus at its high-frequency plateau, while the characteristic relaxation time of the Maxwell model is denoted as τ. The characteristic relaxation time is equal to the value of ω^{-1}, with ω being the angular frequency of the G′-G″ crossover..

The storage modulus, G′, and the loss modulus, G″, were collected as a function of temperature from 15 °C to 55 °C with a heating rate of 1 °C/min to determine the gel point. The gel point is typically defined as the temperature at which a viscous solution transforms into a viscoelastic gel. The gel point can be identified by analyzing the variations in G' and G" as a function of temperature and angular frequency, ω, in the linear viscoelastic regime. According to the Winter and Chambon criterion [51], gelation is reached when G" and G' are both proportional to ωˆn, where n is the relaxation exponent. However, in this study, the gel point was qualitatively identified by the G'-G" crossover temperature at a fixed ω of 10 rad/s.

2.5. Small-angle X-ray scattering (SAXS)

SAXS measurements were conducted using the Xenocs XEUSS 3.0 system (Xenocs SA, Sassenage, France). The scattering intensity, I(q), was recorded with the 2D Pilatus detector (Dectris Ltd, Baden, Switzerland), positioned at 1800 mm from the sample, providing a scattering vector range of $0.015\,Å^{-1} < q < 0.15\,Å^{-1}$. The samples were loaded into disposable 1.5 mm diameter quartz capillaries and then sealed (Hilgenberg GmbH, Malsfeld, Germany). The exposure time was fixed at 2400 s. A Peltier system was used to control the temperature, which was set to 15 °C and 37 °C. The two-dimensional (2D) scattering pattern was radially averaged using SasView software (https://www.sasview.org/) to obtain *I(q)*. The measured scattering curves were corrected for background scattering.

2.6. Dynamic light scattering (DLS)

The DLS measurements were performed using the Zetasizer Nano ZS instrument (Malvern Instruments, Ltd., Worcestershire, UK), which was equipped with a 4 mW He − Ne laser, an automatic laser attenuator, and an avalanche photodiode detector. The measurements were taken at an angle of θ = 173°, and the temperature was set to 20 °C. The autocorrelation functions of the scattered intensity were converted into size measurements using the non-negatively constrained least-squares analysis (general-purpose mode), with the regularizer parameter fixed at 0.01 for all samples. The size distributions were reported based on volume-weighted measurements. The viscosity of the medium was set to that of water, which is 0.08872 mPa·s, with a refractive index of 1.33.

2.7. In vitro drug release

The *in vitro* release study of CEX from P407CS-CiCD and P407CS-CEX was conducted after gelation of 1.4 mL of the P407CS-CiCD and P407CS-CEX formulations, which contained 1.27 mg CEX, at 37 °C. Then, 26.6 mL of a solution of 25 mM phosphate buffer at pH 7.4, containing 2.5 % w/v of HP-β-CD, was added on top. HP-β-CD was added to prevent the precipitation of released CEX due to its low aqueous solubility. The *in vitro* drug release studies were performed in an orbital shaker at 37 °C with an agitation of 100 rpm. At predetermined time intervals of 0, 15, 30, 60, 120, 180, 240, 300, 360, 1440, and 2880 min, 1 mL aliquots were withdrawn and replaced with fresh buffer. The aliquots were then analyzed using High-Performance Liquid Chromatography (HPLC) to estimate the drug content in the acceptor medium. For the HPLC analysis, an Agilent Station was used, consisting of a 1260 Infinity Quaternary LC System equipped with a variable wavelength UV detector, a Rheodyne injector (Rheodyne, Model 7725i) equipped with a 20 μL loop, and OpenLAB CDS ChemStation software (Agilent, Santa Clara, CA). A reverse-phase Column Zorbax C18 Plus (5 μm particle size; 4.6 × 250 mm, Agilent) was chosen as the solid phase. The mobile phase consisted of a mixture (85/15 V/V) of methanol and water (HPLC grade) with 0.1 % V/V of trifluoroacetic acid (TFA) added. The flow rate was set

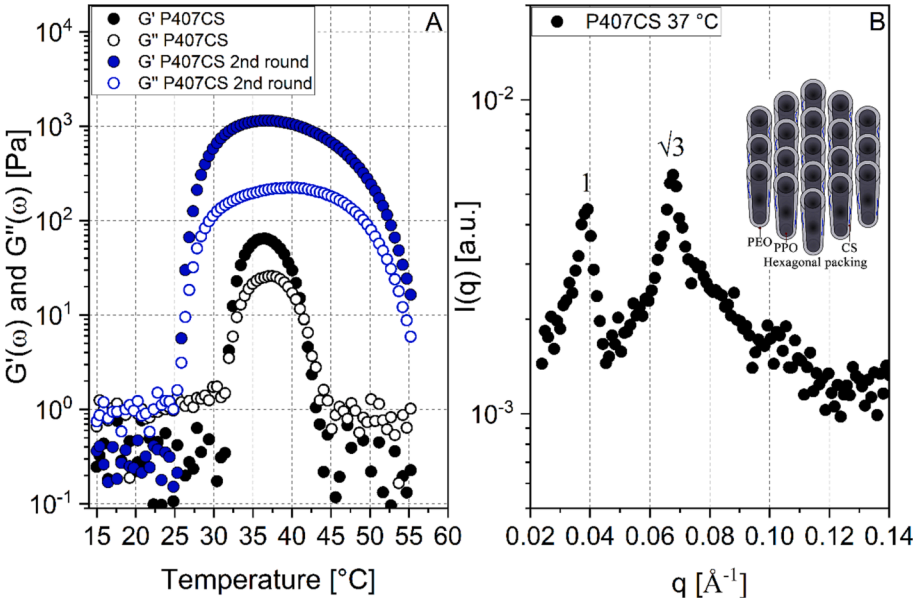

Fig. 2. Dynamic temperature sweep tests were conducted to study the storage modulus, G′, and loss modulus, G″, as a function of the temperature for Poloxamer 407 (P407) at 16 wt% blended with 0.5 wt% of Chitosan (CS) in a 1 wt% aqueous solution of acetic acid (P407CS). The black color represents the first temperature ramp up, while the blue color represents the second temperature ramp up after cooling (A). Additionally, small-angle X-ray scattering intensity, *I(q)*, was measured as a function of the scattering wave vector, *q*, for P407CS at 37 °C after the second dynamic temperature ramp up test (B).

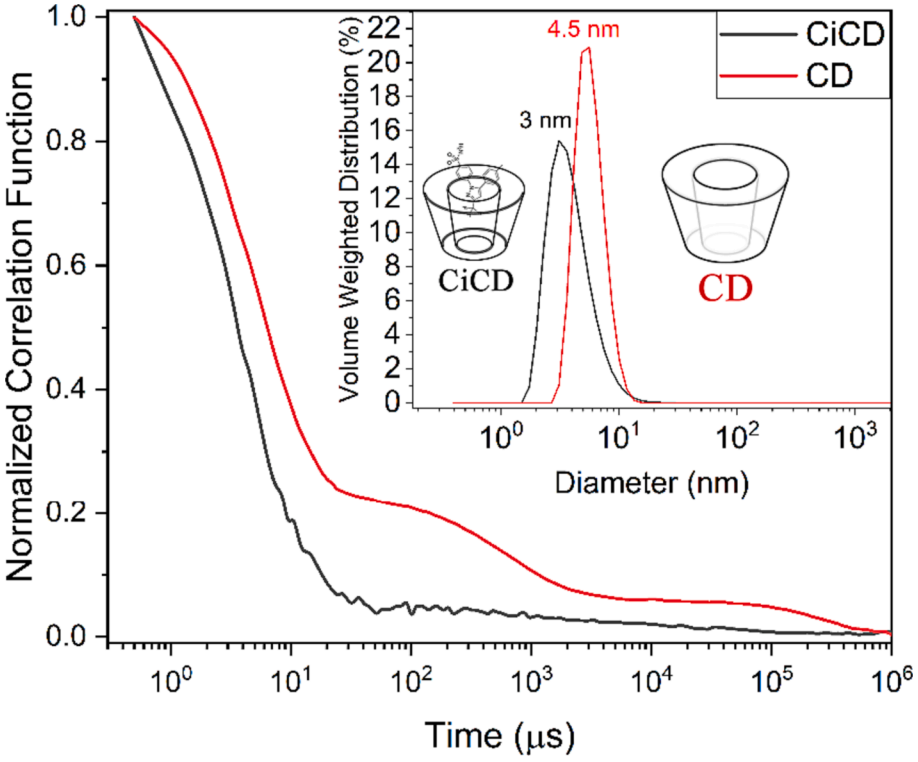

Fig. 3. The normalized autocorrelation functions of the scattered intensity of HP-β-CD (CD) and the Celecoxib-CD inclusion complex at 20 °C is shown, while the inset displays the corresponding volume-weighted size distribution.

at 1.0 mL/min, and the run time was 10 min with an oven temperature of 35 °C and a detection wavelength of 251 nm. A linear calibration curve was obtained by dissolving a known amount of CEX in methanol (1 mg/mL) and progressively diluting it, resulting in a calibration curve in the range of 65.2–0.652 μg/mL ($R^2 = 0.9997$).

3. Results and discussion

3.1. pH effect on the P407 thermogelation

The order–disorder transition of Poloxamer 407 (P407) in water results in gel formation at body temperature, 37 °C, across a wide range of concentrations [10,11,14,20,52]. In the frequency sweep of P407 at 16 wt% in water at 15 °C, a predominant loss modulus, G″, is observed

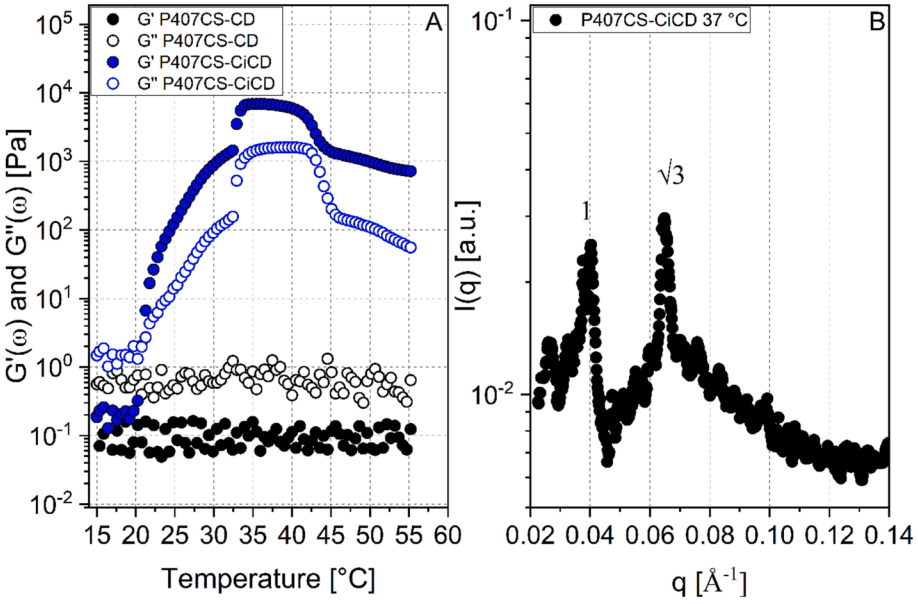

Fig. 4. Dynamic temperature sweep tests with storage modulus, G′, and loss modulus, G″, as a function of the temperature ramp-up of Poloxamer 407 (P407) at 16 wt % blended with 0.5 wt% of Chitosan (CS) in 1 wt% aqueous solution of acetic acid and 1.68 wt% cyclodextrin (P407CS-CD) or Celecoxib-CD inclusion complex (P407CS-CiCD), represented by black and blue colors respectively (A). The small-angle X-ray scattering intensity, *I(q)*, as a function of the scattering wave vector, *q*, for P407CS-CiCD is collected at 37 °C after the dynamic temperature ramp-up test (B).

due to the disordered (isotropic micellar) phase (Fig. 1A) recognised by SAXS analysis (Fig. S1). At 25 °C, interactions between micelles increase, leading to a slightly viscoelastic (weak gel) behavior with a relaxation time of $\tau = \omega^{-1} = 0.11$ s. Further increasing the temperature to 37 °C results in a strong viscoelastic behavior with $\tau = 0.83$ s, and both G′ and G″ moduli are significantly higher compared to 25 °C. As the temperature rises, the hydrophilic chains of the copolymer undergo desolvation, promoting hydrophobic interactions among the PPO domains, thereby contributing to gel formation (ordered phase). This phenomenon is typically characterized by the PPO block becoming more dehydrated, leading to micellar growth and subsequent micellar aggregate formation before transitioning into the gel cubic phase [53]. Hence, the gel transition is attributed to micellar growth and the subsequent bridging of long PEO chains, resulting in increased attractive inter-micellar interactions and the formation of micellar aggregates [54–56]. The temperature sweep test reveals the G′-G″ crossover as a function of the temperature of the P407 at 16 wt% in water leading to a sol–gel transition of 30.5 °C, Fig. 1B. Here, the G′-G″ crossover as a function of temperature is considered qualitatively as the sol–gel transition temperature. All these rheological data are perfectly in agreement with the literature [11]. The corresponding 1D-SAXS profile of P407 at 16 wt% at 37 °C shows a series of peaks with ratios of peak positions characteristic of an FCC phase [19]. However, this well-documented transition from isotropic micelles to the FCC phase can be influenced by pH [57–60]. Nevertheless, most of the literature focuses on the effect of pH concerning a drug in a P407 matrix. In this study, we primarily focus on the effect of pH on P407. A first dynamic temperature sweep test was performed on the P407 16 wt% in a 1 wt% aqueous solution of acetic acid with an acidic pH of 3.1, contrasting with a pH of 7.1 in water (Table 1). The test was conducted from 15 °C to 55 °C (ramp up) and resulted in a G′-G″ crossover at 38 °C, as shown in the green profile in Fig. 1B. The frequency sweep experiments conducted on the P407Ac 16 wt% provided consistent results with the temperature tests, providing insight into the gel phase. Specifically, the G′ and G″ moduli were two orders of magnitude lower compared to the corresponding sample in water at pH 7.1 (Fig. 1C). The sample was then cooled down, and a second temperature ramp-up test (green profile) was performed, leading to a G′-G″ crossover at 35.5 °C. The lower temperature of the crossover value is attributed to water evaporation, resulting in higher acetic acid concentration. The different rheological behavior is attributed to a structural change, identifiable by the 1D SAXS profiles, which revealed a lamellar phase in the presence of acetic acid at 37 °C instead of the FCC phase observed in water at the same temperature (Fig. 1D).

Fasolin et al., while studying the impact of short-chain organic acids as co-surfactants in microemulsions, noted that acetic acid was more susceptible to dissociation due to its higher polarity, reducing its presence near the oil–water interface [61]. Here, the phase behavior of P407 containing acetic acid is divergent from P407 with acetic acid differs from that of P407 in pure water, possibly due to the surface-active properties of acetic acid. Therefore, the interactions between the polymer chains, as well as between the polymer aggregates, are less favored, and the gelation process occurs at higher temperatures.

3.2. P407-Chitosan blended system

Chitosan (CS) can be blended to enhance the adhesive properties of Poloxamer 407 in the presence of acetic acid, which is needed to solubilize CS [32,62]. In the P407CS 16 wt% blend containing 0.5 wt% chitosan in 1 wt% acetic acid, the G′-G″ crossover temperature decreases to 25.8 °C compared to the first temperature ramp up where the crossover was located at 31.9 °C (Fig. 2A), due to the evaporation of acetic acid as observed in paragraph 3.1. The transition temperature is also lower than the previous P407 in water alone, with G′ and G″ moduli one order of magnitude lower. The structural changes due to the presence of CS are confirmed by the 1D SAXS profiles, where a hexagonal packing can be appreciated at 37 °C (Fig. 2B).

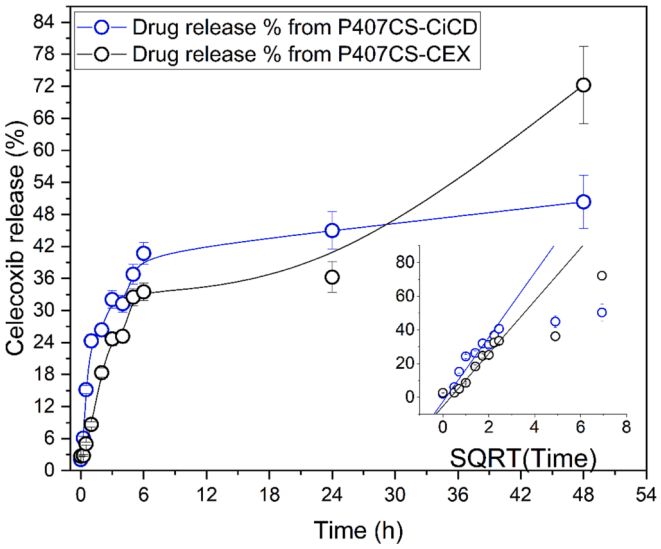

Fig. 5. The release profile of celecoxib from the inclusion complex entrapped in the P407CS at 16 wt% of P407 and 0.5 wt% of chitosan in an aqueous solution of 1 wt% acetic acid (P407CS-CiCD) and celecoxib in the P407CS (P407CS-CEX) matrix in the absence of the inclusion complex is shown in the figure. The lines are guides for the eyes. The inset is the Higuchi plot, where the straight lines are linear fittings made in the region before 12 h.

3.3. HP-β-CD and the celecoxib inclusion complex

The 2-hydroxypropyl-β-cyclodextrin (HP-β-CD) is commonly used as an excipient in pharmaceutical formulations due to its ability to form inclusion complexes with poorly soluble drugs such as Celecoxib [63,64]. The shape of β-CD is well-represented by a truncated cone rather than perfect cylinders, owing to the chair conformation of the glucopyranose units. The hydroxyl functions, including the 2-HP groups of the HP-β-CD derived are oriented to the cone exterior, making its outer surface hydrophilic, while the central cavity is lined with the skeletal carbons and ethereal oxygen of the glucose residues, imparting a lipophilic character [65,66]. For this reason the DCs (host) are used to form inclusion complexes with lipophilic molecules (guest) called host–guest complexes. To investigate the effect of HP-β-CD (indicated simply as CD) and the Celecoxib-CD inclusion complex (CiCD) on the P407CS blend, dynamic light scattering measurements were performed on the CD and CiCD in an aqueous solution of 1 wt% acetic acid.

Fig. 3 shows the correlation functions of the scattered intensity of the CD and CiCD in aqueous solutions of 1 wt% acetic acid at 20 °C, where the CiCD correlation function decays much faster than that of CD. Moreover, the CD correlation function is clearly represented by multiple decays, which may be due to impurities or aggregates. The volume-weighted distributions provide a good description of the systems by minimizing the influence of a few larger aggregates. The CD in the aqueous solution of 1 wt% acetic acid shows a distribution centered at 4.5 nm. The diameter is in agreement with the HP-β-CD samples with a degree of substitution of ~ 6 [64], which is consistent with the hydrodynamic diameter corresponding approximately to the geometrical diameter of a single β-CD molecule. On the other hand, the CiCD presents a distribution centered at 3 nm due to the interaction between the CD cavity and the Celecoxib molecule. The intensity-weighted size distributions (Fig. S2) align with the volume-weighted size distributions discussed, yet they also showcase a multimodal distribution, as anticipated from the non-monoexponential decay observed in the correlation functions. This occurrence is likely due to a few cyclodextrin aggregates, as documented in the literature [46].

3.4. Celecoxib inclusion complex in the P407-Chitosan matrix

The presence of the Celecoxib-CD inclusion complex (CiCD) in the P407CS matrix with 16 wt% of P407 (P407CS-CiCD) decreases the G′-G″ crossover temperature to 25.8 °C, which is the same value obtained for the corresponding chitosan blend (P407CS) in the aqueous solution of 1 wt% acetic acid. This indicates almost no effect on the thermogelation process. Surprisingly, the presence of CD alone in the P407CS (P407CS-CD) leads to no order–disorder transition, meaning no gelation process as a function of temperature, with G″ always higher than G′ in the overall temperature range investigated (Fig. 4A). The CD might interact with the PPO fraction of the P407, preventing, or partially preventing, the self-assembly of the polymeric micelles. This evidence is supported by previous work on similar systems [44,47]. However, after acetic acid evaporation, the CS is no longer solubilized in the system, CD interacts with CS, and the gel formation reappears (Fig. S3 in the supporting information). The 1D SAXS profile of the P407CS-CiCD system at 37 °C (Fig. 4B) shows no changes compared to the P407CS (Fig. 2B), indicating the presence of a hexagonal packing.

3.5. Celecoxib release

The release profile of CEX from P407CS-CiCD and P407CS-CEX (Fig. 5) was investigated to evaluate how the presence of HP-β-CD and the consequent formation of the inclusion complex affects the release of the drug from the gel. Both formulations show the same behavior with continuous release of CEX over time. The partial release of the drug resulted in a maximum value of 44.99 % from P407CS-CiCD and 36.26 % from P407CS-CEX after 24 h. After 48 h, a 50.36 % release of CEX from the P407CS-CiCD formulation is observed compared to the 72.00 % release of CEX obtained from the P407CS-CEX formulation. The release of CEX from the P407CS-CiCD and P407CS-CEX is regulated in the first stage by the diffusion through the polymer matrix, which provides a constant release as a function of time. The experimental data were plotted using the Higuchi square-root equation [67]. The high values obtained for the correlation coefficients from P407CS-CiCD (R^2 = 0.9857) and P407CS-CEX (R^2 = 0.9803) confirmed that, for both formulations, the kinetic release of CEX was controlled by a diffusion process in the initial stage. In the final stage the matrix network is now retained anymore and the release is regulated by the inclusion complex in the case of the first formulation (P407CS-CiCD), while the drug is free in the second formulation (P407CS-CEX), allowing a higher release. The raw data on the release profile are reported in Table S1 (supporting information).

4. Conclusions

In the presence of Poloxamer 407 at 16 wt%, a gel is formed at 30.5 °C, transitioning from an initial isotropic micellar solution in water with a pH of 7.1 to a face-centered cubic phase (FCC). However, the addition of acetic acid (pH of 3.1) significantly alters the gelation process. The formation of a lamellar phase instead of the FCC phase is most likely due to the surface-active properties of acetic acid, which acts as a co-surfactant. From an application perspective, the assembly of the lamellar phase is preferred due to its injectability. Moreover, after acetic acid evaporation, the resulting gel exhibits a higher storage modulus.

When chitosan is blended with Poloxamer 407, a hexagonal phase is observed at 37 °C, indicating a distinct structural arrangement. The impact of 2-hydroxypropyl-β-cyclodextrin (HP-β-CD), termed CD, and the celecoxib inclusion complex (CiCD) on the P407CS system is studied using rheology and small-angle X-ray scattering (SAXS). CD hinders gelation by interacting with the hydrophobic PPO unit of P407. In contrast, CiCD does not significantly affect the P407CS structure. Dynamic light scattering data on CD and CiCD in acetic acid solutions reveal that CD's dimensions are larger than CiCD's due to interactions between CD and the hydrophobic celecoxib.

These findings confirm our hypothesis that incorporating HP-β-CD and the celecoxib-HP-β-CD inclusion complex into a 16 wt% P407 and chitosan blend in an aqueous acetic acid solution affects the system's rheological and structural properties.

Regarding celecoxib release, the P407CS-CiCD system demonstrates a partial release of celecoxib, reaching a maximum of approximately 50 % after 48 h. In contrast, without the inclusion complex, around 72 % of the drug is released. Initially, release is attributed to polymer matrix diffusion, while after 24 h, when the matrix gel is no longer retained, the release is regulated by the presence of the inclusion complex or the free drug.

CRediT authorship contribution statement

Valentino Laquintana: . **Angela A. Lopedota:** Investigation, Methodology, Resources. **Marianna Ivone:** Investigation, Methodology. **Nunzio Denora:** Resources, Validation. **Massimo Franco:** Resources, Validation. **Gerardo Palazzo:** . **Luigi Gentile:** .

Declaration of competing interest

The authors declare that they have no known competing financial interests or personal relationships that could have appeared to influence the work reported in this paper.

Data availability

Data will be made available on request.

Acknowledgments

We gratefully acknowledge the support of CSGI (Consorzio Interuniversitario per lo Sviluppo dei Sistemi a Grande Interfase).

Appendix A. Supplementary material

Supplementary data to this article can be found online at https://doi.org/10.1016/j.jcis.2024.01.019.

References

[1] N. Raval, D. Kalyane, R. Maheshwari, R.K. Tekade, Copolymers and Block Copolymers in Drug Delivery and Therapy, Basic Fundamentals Drug Deliv. (2019) 173–201. Doi: 10.1016/B978-0-12-817909-3.00005-4.
[2] A.P. Dabkowska, C. Hirst, M. Valldeperas, L.A. Clifton, C. Montis, S. Nöjd, L. Gentile, M. Wang, G.K. Pálsson, S. Lages, D. Berti, J. Barauskas, T. Nylander, Temperature responsive lipid liquid crystal layers with embedded nanogels, Chem. Commun. 53 (2017), https://doi.org/10.1039/c6cc09426k.
[3] E. Tasca, P. Andreozzi, A. Del Giudice, L. Galantini, K. Schillén, A. Maria Giuliani, M. de los A. Ramirez, S.E. Moya, M. Giustini, Poloxamer/sodium cholate co-formulation for micellar encapsulation of doxorubicin with high efficiency for intracellular delivery: An in-vitro bioavailability study, J. Colloid Interface Sci. 579 (2020) 551–561, https://doi.org/10.1016/j.jcis.2020.06.096.
[4] D. Tatini, P. Tempesti, F. Ridi, E. Fratini, M. Bonini, P. Baglioni, Pluronic/gelatin composites for controlled release of actives, Colloids Surf. B Biointerfaces 135 (2015) 400–407, https://doi.org/10.1016/J.COLSURFB.2015.08.002.
[5] A.M. Bodratti, P. Alexandridis, Formulation of poloxamers for drug delivery, J. Functional Biomater. 9 (2018) 11, https://doi.org/10.3390/jfb9010011.
[6] A.V. Kabanov, P. Lemieux, S. Vinogradov, V. Alakhov, Pluronic® block copolymers: novel functional molecules for gene therapy, Adv. Drug Deliv. Rev. 54 (2002) 223–233, https://doi.org/10.1016/S0169-409X(02)00018-2.
[7] F.E. Antunes, L. Gentile, C. Oliviero Rossi, L. Tavano, G.A. Ranieri, Gels of Pluronic F127 and nonionic surfactants from rheological characterization to controlled drug permeation, Colloids Surf. B Biointerfaces 87 (2011), https://doi.org/10.1016/j.colsurfb.2011.04.033.
[8] B. Shriky, A. Kelly, M. Isreb, M. Babenko, N. Mahmoudi, S. Rogers, O. Shebanova, T. Snow, T. Gough, Pluronic F127 thermosensitive injectable smart hydrogels for controlled drug delivery system development, J. Colloid Interface Sci. 565 (2020) 119–130, https://doi.org/10.1016/J.JCIS.2019.12.096.
[9] K. Mortensen, W. Brown, E. Jørgensen, Phase Behavior of Poly(propylene oxide)-Poly(ethylene oxide)-Poly(propylene oxide) Triblock Copolymer Melt and Aqueous Solutions, Macromolecules 27 (1994) 5654–5666, https://doi.org/10.1021/MA00098A020/ASSET/MA00098A020.FP.PNG_V03.

[10] P. Alexandridis, T. Alan Hatton, Poly(ethylene oxide)poly(propylene oxide)poly (ethylene oxide) block copolymer surfactants in aqueous solutions and at interfaces: thermodynamics, structure, dynamics, and modeling, Colloids Surf. A Physicochem. Eng. Asp 96 (1995) 1–46, https://doi.org/10.1016/0927-7757(94)03028-X.
[11] L. Gentile, G. De Luca, F.E. Antunes, C.O. Rossi, G.A. Ranieri, Thermogelation analysis of F127-water mixtures by physical Chemistry techniques, Appl. Rheol. 20 (2010) 1–12, https://doi.org/10.3933/ApplRheol-20-52081.
[12] A.F. Sepulveda, M. Kumpgdee-Vollrath, M.K.K.D. Franco, F. Yokaichiya, D.R. de Araujo, Supramolecular structure organization and rheological properties modulate the performance of hyaluronic acid-loaded thermosensitive hydrogels as drug-delivery systems, J. Colloid Interface Sci. 630 (2023) 328–340, https://doi.org/10.1016/j.jcis.2022.10.064.
[13] R. Ivanova, B. Lindman, P. Alexandridis, Evolution in structural polymorphism of Pluronic F127 poly(ethylene oxide)-poly(propylene oxide) block copolymer in ternary systems with water and pharmaceutically acceptable organic solvents: From 'glycols' to 'oils', Langmuir 16 (2000) 9058–9069, https://doi.org/10.1021/LA000373D/ASSET/IMAGES/LARGE/LA000373DF00009.JPEG.
[14] G. Wanka, H. Hoffmann, W. Ulbricht, Phase Diagrams and Aggregation Behavior of Poly(oxyethylene)-Poly(oxypropylene)-Poly(oxyethylene) Triblock Copolymers in Aqueous Solutions, Macromolecules 27 (1994) 4145–4159, https://doi.org/10.1021/MA00093A016/ASSET/MA00093A016.FP.PNG_V03.
[15] M. Malmsten, B. Lindman, Effects of Homopolymers on the Gel Formation in Aqueous Block Copolymer Solutions, Macromolecules 26 (1993) 1282–1286, https://doi.org/10.1021/ma00058a014.
[16] Y. Li, R. Xu, D.M. Bloor, J.F. Holzwarth, E. Wyn-Jones, Binding of sodium dodecyl sulfate to the ABA block copolymer pluronic F127 (EO97PO69EO97): An electromotive force, microcalorimetry, and light scattering investigation, Langmuir 16 (2000) 10515–10520, https://doi.org/10.1021/LA000899Y/ASSET/IMAGES/LARGE/LA000899YF00006.JPEG.
[17] S. Bayati, C. Anderberg Haglund, N.V. Pavel, L. Galantini, K. Schillén, Interaction between bile salt sodium glycodeoxycholate and PEO–PPO–PEO triblock copolymers in aqueous solution, RSC Adv. 6 (2016) 69313–69325, https://doi.org/10.1039/C6RA12514J.
[18] R.K. Prud'homme, G. Wu, D.K. Schneider, Structure and rheology studies of poly (oxyethylene-oxypropylene-oxyethylene) aqueous solution, Langmuir 12 (1996) 4651–4659, https://doi.org/10.1021/la951506b.
[19] H.S. Jang, T.H. Kim, C. Do, M.J. Lee, S.M. Choi, Single-walled carbon nanotube induced re-entrant hexagonal phases in a Pluronic block copolymer system, Soft Matter 9 (2013) 3050–3056, https://doi.org/10.1039/C3SM27589B.
[20] K. Mortensen, W. Batsberg, S. Hvid, Effects of PEO-PPO diblock impurities on the cubic structure of aqueous PEO-PPO-PEO pluronics micelles: Fee and bcc ordered structures in F127, Macromolecules 41 (2008) 1720–1727, https://doi.org/10.1021/MA702269C/ASSET/IMAGES/LARGE/MA702269CF00009.JPEG.
[21] J. Zhang, C. Burger, B. Chu, Nanostructured polymer matrix for oligonucleotide separation, Electrophoresis 27 (2006) 3391–3398, https://doi.org/10.1002/ELPS.200500839.
[22] A.W. Kirkeminde, T. Torres, T. Ito, D.A. Higgins, Multiple diffusion pathways in pluronic F127 mesophases revealed by single molecule tracking and fluorescence correlation spectroscopy, J. Phys. Chem. B 115 (2011) 12736–12743, https://doi.org/10.1021/jp208234b.
[23] W. Brown, K. Schillén, S. Hvidt, Triblock copolymers in aqueous solution studied by static and dynamic light scattering and oscillatory shear measurements. Influence of relative block sizes, J. Phys. Chem. 96 (1992) 6038–6044, https://doi.org/10.1021/J100193A072/ASSET/J100193A072.FP.PNG_V03.
[24] R. Basak, N. Mukhopadhyay, R. Bandyopadhyay, Experimental studies of the jamming behaviour of triblock copolymer solutions and triblock copolymer-anionic surfactant mixtures, The European Physical Journal, E, Soft Matter. 34 (2011) 103, https://doi.org/10.1140/EPJE/I2011-11103-Y.
[25] T. Thurn, S. Couderc, J. Sidhu, D.M. Bloor, J. Penfold, J.F. Holzwarth, E. Wyn-Jones, Study of mixed micelles and interaction parameters for ABA triblock copolymers of the type EOm-POn-EOm and ionic surfactants: Equilibrium and structure, Langmuir 18 (2002) 9267–9275, https://doi.org/10.1021/LA020629A/ASSET/IMAGES/LARGE/LA020629AF00011.JPEG.
[26] J. Jansson, K. Schillén, G. Olofsson, R.C. Da Silva, W. Loh, Interaction between PEO-PPO-PEO triblock copolymers and ionic surfactants in aqueous solution studied using light scattering and calorimetry, J. Phys. Chem. B 108 (2004) 82–92, https://doi.org/10.1021/JP030792U/ASSET/IMAGES/LARGE/JP030792UF00009.JPEG.
[27] P.R. Desai, N.J. Jain, R.K. Sharma, P. Bahadur, Effect of additives on the micellization of PEO/PPO/PEO block copolymer F127 in aqueous solution, Colloids Surf. A Physicochem. Eng. Asp 178 (2001) 57–69, https://doi.org/10.1016/S0927-7757(00)00493-3.
[28] V.P. Torchilin, Structure and design of polymeric surfactant-based drug delivery systems, J. Control. Release 73 (2001) 137–172, https://doi.org/10.1016/S0168-3659(01)00299-1.
[29] F. Ricci, G.F. Racaniello, N. Denora, L. Gentile, A. Lopalco, A. Cutrignelli, M. Franco, R.M. Iacobazzi, V. Laquintana, A. Lopedota, Thermoresponsive mucoadhesive hydrogel based on Pluronic F127/thiolated glycol chitosan for intravesical administration of celecoxib/gemcitabine, J. Drug Delivery Sci. Technol. 86 (2023) 104687, https://doi.org/10.1016/J.JDDST.2023.104687.
[30] F. Comblain, G. Rocasalbas, S. Gauthier, Y. Henrotin, Chitosan: A promising polymer for cartilage repair and viscosupplementation, Biomed. Mater. Eng. 28 (2017) S209–S215, https://doi.org/10.3233/BME-171643.
[31] A.H. Salama, A.A. Abdelkhalek, N.A. Elkasabgy, Etoricoxib-loaded bio-adhesive hybridized polylactic acid-based nanoparticles as an intra-articular injection for the treatment of osteoarthritis, Int. J. Pharm. 578 (2020) 119081, https://doi.org/10.1016/J.IJPHARM.2020.119081.
[32] T. Ur-Rehman, S. Tavelin, G. Gröbner, Chitosan in situ gelation for improved drug loading and retention in poloxamer 407 gels, Int. J. Pharm. 409 (2011) 19–29, https://doi.org/10.1016/J.IJPHARM.2011.02.017.
[33] J. García-Couce, M. Tomás, G. Fuentes, I. Que, A. Almirall, L.J. Cruz, Chitosan/Pluronic F127 Thermosensitive Hydrogel as an Injectable Dexamethasone Delivery Carrier, Gels. 8 (2022), https://doi.org/10.3390/GELS8010044.
[34] T. Loftsson, D. Hreinsdóttir, M. Másson, Evaluation of cyclodextrin solubilization of drugs, Int. J. Pharm. 302 (2005) 18–28, https://doi.org/10.1016/J.IJPHARM.2005.05.042.
[35] T. Loftsson, M.E. Brewster, Cyclodextrins as functional excipients: methods to enhance complexation efficiency, J. Pharm. Sci. 101 (2012) 3019–3032, https://doi.org/10.1002/JPS.23077.
[36] T. Kataoka, M. Kidowaki, C. Zhao, H. Minamikawa, T. Shimizu, K. Ito, Local and Network Structure of Thermoreversible Polyrotaxane Hydrogels Based on Poly (ethylene glycol) and Methylated $α$-Cyclodextrins, J. Phys. Chem. B 110 (2006) 24377–24383, https://doi.org/10.1021/JP0649246.
[37] G. Bonacucina, M. Spina, M. Misici-Falzi, M. Cespi, S. Pucciarelli, M. Angeletti, G. F. Palmieri, Effect of hydroxypropyl beta-cyclodextrin on the self-assembling and thermogelation properties of Poloxamer 407, Eur. J. Pharmaceut. Sci.: Off. J. Eur. Federation Pharmaceut. Sci. 32 (2007) 115–122, https://doi.org/10.1016/J.EJPS.2007.06.004.
[38] L. Nogueiras-Nieto, E. Sobarzo-Sánchez, J.L. Gómez-Amoza, F.J. Otero-Espinar, Competitive displacement of drugs from cyclodextrin inclusion complex by polypseudorotaxane formation with poloxamer: implications in drug solubilization and delivery, Eur. J. Pharmaceut. Biopharmaceut.: Off. J. Arbeitsgemeinschaft Fur Pharmazeutische Verfahrenstechnik E.v. 80 (2012) 585–595, https://doi.org/10.1016/J.EJPB.2011.12.001.
[39] C. Pradal, K.S. Jack, L. Grøndahl, J.J. Cooper-White, Gelation kinetics and viscoelastic properties of pluronic and α-cyclodextrin-based pseudopolyrotaxane hydrogels, Biomacromolecules 14 (2013) 3780–3792, https://doi.org/10.1021/BM401168H/SUPPL_FILE/BM401168H_SI_001.PDF.
[40] C. Di Donato, R. Iacovino, C. Isernia, G. Malgieri, A. Varela-Garcia, A. Concheiro, C. Alvarez-Lorenzo, Polypseudorotaxanes of Pluronic® F127 with Combinations of α- and β-Cyclodextrins for Topical Formulation of Acyclovir, Nanomaterials 10 (2020), https://doi.org/10.3390/NANO10040613.
[41] S.M.N. Simões, F. Veiga, A.C.F. Ribeiro, A.R. Figueiras, P. Taboada, A. Concheiro, C. Alvarez-Lorenzo, Supramolecular gels of poly-α-cyclodextrin and PEO-based copolymers for controlled drug release, Eur. J. Pharmaceut. Biopharmaceut.: Off. J. Arbeitsgemeinschaft Fur Pharmazeutische Verfahrenstechnik E.v. 87 (2014) 579–588, https://doi.org/10.1016/J.EJPB.2014.04.006.
[42] M.M. Calvino, G. Lazzara, G. Cavallaro, S. Milioto, Inclusion complexes of triblock L35 copolymer and hydroxyl propyl cyclodextrins: a physico-chemical study, New J. Chem. 46 (2022) 6114–6120, https://doi.org/10.1039/D2NJ00486K.
[43] M. Kkd Franco, Budesonide-Hydroxypropyl-$β$-Cyclodextrin Inclusion Complex in Poloxamer 407 and Poloxamer 407/403Systems: A Structural Study by Small Angle X-Ray Scattering (SAXS), Biomed. J. Sci. Tech. Res. 10 (2018), https://doi.org/10.26717/bjstr.2018.10.002002.
[44] G. Lazzara, S. Milioto, Copolymer-cyclodextrin inclusion complexes in water and in the solid state. A Physico-Chemical Study, J. Phys. Chem. b. 112 (2008) 11887–11895, https://doi.org/10.1021/JP8034924/SUPPL_FILE/JP8034924_SI_001.PDF.
[45] R. De Lisi, G. Lazzara, Aggregation in aqueous media of tri-block copolymers tuned by the molecular selectivity of cyclodextrins, J. Therm. Anal. Calorim. 97 (2009) 797–803, https://doi.org/10.1007/S10973-009-0223-0/FIGURES/7.
[46] G. Lazzara, G. Olofsson, V. Alfredsson, K. Zhu, B. Nyström, K. Schillén, Temperature-responsive inclusion complex of cationic PNIPAAM diblock copolymer and γ-cyclodextrin, Soft Matter 8 (2012) 5043–5054, https://doi.org/10.1039/C2SM07252A.
[47] M. Valero, W. Hu, J.E. Houston, C.A. Dreiss, Solubilisation of salicylate in F127 micelles: Effect of pH and temperature on morphology and interactions with cyclodextrin, J. Mol. Liq. 322 (2021) 114892, https://doi.org/10.1016/J.MOLLIQ.2020.114892.
[48] L. Gentile, S. Amin, Rheology primer for nanoparticle scientists, Colloidal Foundations Nanosci. (2022) 289–306, https://doi.org/10.1016/b978-0-12-822089-4.00003-9.
[49] J.D. Ferry, Viscoelastic properties of polymers, 3rd edition,, Wiley, New York, 1980, p. 672.
[50] T.G. Mezger, The Rheology Handbook, Vincentz Network, Hannover, 2009. Doi: 10.1108/prt.2009.12938eac.006.
[51] H.H. Winter, F. Chambon, Analysis of Linear Viscoelasticity of a Crosslinking Polymer at the Gel Point, J. Rheol. 30 (1986) 367–382, https://doi.org/10.1122/1.549853.
[52] S.Y. Park, Y. Lee, K.H. Bae, C.H. Ahn, T.G. Park, Temperature/pH-sensitive hydrogels prepared from pluronic copolymers end-capped with carboxylic acid groups via an oligolactide spacer, Macromol. Rapid Commun. 28 (2007) 1172–1176, https://doi.org/10.1002/MARC.200600914.
[53] O. Glatter, G. Scherf, K. Schillén, W. Brown, Characterization of a Poly(ethylene oxide)-Poly(propylene oxide) Triblock Copolymer (EO27-PO39-EO27) in Aqueous Solution, Macromolecules 27 (1994) 6046–6054, https://doi.org/10.1021/MA00099A017/ASSET/MA00099A017.FP.PNG_V03.
[54] S.C. Miller, B.R. Drabik, Rheological properties of poloxamer vehicles, Int. J. Pharm. 18 (1984) 269–276, https://doi.org/10.1016/0378-5173(84)90142-X.

[55] D. Attwood, J.H. Collett, C.J. Tait, The micellar properties of the poly(oxyethylene) - poly(oxypropylene) copolymer Pluronic F127 in water and electrolyte solution, Int. J. Pharm. 26 (1985) 25–33, https://doi.org/10.1016/0378-5173(85)90197-8.
[56] K. Schillén, W. Brown, C. Koňák, Aggregation of a Polyethylene oxide)–Poly (propylene oxide)–Poly(ethylene oxide) Triblock Copolymer in Aqueous Solution Studied Using Rayleigh-Brillouin and Dynamic Light Scattering, Macromolecules 26 (1993) 3611–3614, https://doi.org/10.1021/MA00066A020/ASSET/MA00066A020.FP.PNG_V03.
[57] L.E. Nita, A.P. Chiriac, M. Bercea, Effect of pH and temperature upon self-assembling process between poly(aspartic acid) and Pluronic F127, Colloids Surf. B Biointerfaces 119 (2014) 47–54, https://doi.org/10.1016/J.COLSURFB.2014.04.023.
[58] S. Chatterjee, P.C. leung Hui, C. wai Kan, W. Wang, Dual-responsive (pH/temperature) Pluronic F-127 hydrogel drug delivery system for textile-based transdermal therapy, Scientific Reports 2019 9:1. 9 (2019) 1–13. Doi: 10.1038/s41598-019-48254-6.
[59] R. Basak, R. Bandyopadhyay, Encapsulation of hydrophobic drugs in pluronic F127 micelles: Effects of drug hydrophobicity, solution temperature, and pH, Langmuir 29 (2013) 4350–4356, https://doi.org/10.1021/LA304836E/SUPPL_FILE/LA304836E_SI_001.PDF.
[60] E. Brambilla, S. Locarno, S. Gallo, F. Orsini, C. Pini, M. Farronato, D.V. Thomaz, C. Lenardi, M. Piazzoni, G. Tartaglia, Poloxamer-Based Hydrogel as Drug Delivery System: How Polymeric Excipients Influence the Chemical-Physical Properties, Polymers 14 (2022), https://doi.org/10.3390/polym14173624.
[61] L.H. Fasolin, R.C. Santana, R.L. Cunha, Influence of organic acids on surfactant self-assemblies in surfactant/oil/water systems, Colloids Surf A Physicochem Eng Asp 459 (2014) 290–297, https://doi.org/10.1016/J.COLSURFA.2014.07.010.
[62] T. Gratieri, G.M. Gelfuso, E.M. Rocha, V.H. Sarmento, O. de Freitas, R.F.V. Lopez, A poloxamer/chitosan in situ forming gel with prolonged retention time for ocular delivery, 75 (2010) 186–193. Doi: 10.1016/J.EJPB.2010.02.011.
[63] B. Gidwani, A. Vyas, A Comprehensive Review on Cyclodextrin-Based Carriers for Delivery of Chemotherapeutic Cytotoxic Anticancer Drugs, Biomed Res. Int. 2015 (2015), https://doi.org/10.1155/2015/198268.
[64] H.H. Wu, P. Garidel, B. Michaela, HP-β-CD for the formulation of IgG and Ig-based biotherapeutics, Int. J. Pharm. 601 (2021), https://doi.org/10.1016/J.IJPHARM.2021.120531.
[65] S.S. Jambhekar, P. Breen, Cyclodextrins in pharmaceutical formulations I: structure and physicochemical properties, formation of complexes, and types of complex, Drug Discov. Today 21 (2016) 356–362, https://doi.org/10.1016/J.DRUDIS.2015.11.017.
[66] M.E. Davis, M.E. Brewster, Cyclodextrin-based pharmaceutics: past, present and future, Nat. Rev. Drug Discovery 3(12) (2004) 1023–1035. Doi: 10.1038/nrd1576.
[67] T. Higuchi, Mechanism of sustained-action medication. Theoretical analysis of rate of release of solid drugs dispersed in solid matrices, J. Pharm. Sci. 52 (1963) 1145–1149, https://doi.org/10.1002/jps.2600521210.